A STUDY ON COMMON-MODE CURRENT ON FEED CABLE ATTACHED TO PCB WITH DIFFERENT CROSS SECTIONAL STRUCTURES

Yoshiki Kayano, Motoshi Tanaka and Hiroshi Inoue
Faculty of Engineering and Resource Science, Akita University
E-mail: kayano@venus.ee.akita-u.ac.jp

Abstract: Common-mode (CM) current on a feed cable attached to a PCB is investigated experimentally and with numerical calculation. Four kinds of different cross sectional structures of PCBs were employed. Results show that the shield structure is effective in suppressing the CM current at lower frequency. However structure, in which a conductive plate exists near the signal trace, yields resonances with high level peak of CM current. This study can be a basic consideration to realize a technique which is effective on the suppression of the CM current on the PCB with a connected feed cable.
Key words: Common-mode Current, Printed Circuit Board, Electromagnetic interference, FDTD method

1. Introduction

Electronic instruments which have high immunity from the external electromagnetic noise without undesired electromagnetic radiation are required. Many electronic instruments require feed cable for the operation. In the state of an ideal balance, signal and return current in the feed cable are equal. However, for real feed cable, the ideal balance can not be established, and, hence, unbalanced current called common-mode (CM) current exists. CM current is considered as a main source of the radiated electromagnetic interference (EMI) from electronic instruments. So far some studies on the electromagnetic noise radiated from a printed circuit board (PCB) have been published [1]-[3]. It is necessary to suppress the CM current to reduce the radiation. The CM radiation from cables attached to a PCB, as well as radiation from the PCB itself, is a total EMI problem.

The authors have been discussed the CM current on a feed cable due to a trace near a PCB edge by experiment and numerical modeling [4],[5]. In the results, as the trace is moved closer to the PCB edge, CM current increases. The guard-band (GB) which is connected to the whole edge of the ground plane to suppress the CM current in the case of surface micro-strip line structure is proposed.

So far, some design structures of the signal line on the PCB are proposed [6]. The strip line, which is simulated inner transmission line of multilayer PCBs, is investigated by Otsuka and et al. [7]. It was suggested that the strip line that is varied in the dielectric material has smaller radiation and crosstalk. But the research work of the CM current point of view is not thoroughgoing enough.

In this paper, the effect of PCB structure on suppression of CM current is investigated with experiment and FDTD modeling. Four kinds of PCB structures, which are expected as typical structures, are used to compare. First, CM current on the feed cable is discussed. Second, reflection coefficient which is associated with EMI is also discussed experimentally.

2. PCB Structure

The geometry of PCB layout under test is illustrated in Fig. 1. Four different PCB cross sectional structures, as shown in Fig. 2, were prepared for the measurements. (a) is surface micro-strip line structure (S-MSL), (b) is embedded micro-strip line structure (E-MSL), (c) is strip line structure (SL) and (d) is shield structure (Shield). The width w of ground plane, thickness h of dielectric substrate, the width w_t of trace, and the relative permittivity of dielectric substrate all affect the characteristic impedance Z_0 of the trace [6]. In this paper, the size of PCB is 150mm length, 100mm width and 1.53(or 3.06)mm thickness of the dielectric substrate with ε_r=4.5. The trace with 50mm length was centered on dielectric substrate. The sizes are selected for the comparison with our former studies [4],[5]. The w_t was designed so that characteristic impedance Z_0 of the trace was set at 50Ω. In order to match the impedance, the trace was terminated with 51Ω SMT resistor. The PCB was driven through a 0.085"semi-rigid coaxial cable running along the center of the PCB on the reverse side. The cable ran the length of the PCB to the feed point of the driven trace, and was soldered to the ground plane along its entire length. The center conductor of the semi-rigid coaxial cable was extended beyond the outer shield and penetrated the PCB through the ground plane to connect to the trace on the top side. The coaxial cable extended 30mm beyond the PCB edge, and an SMA connector was located at the end of the cable.

The characteristic impedance Z_0 of the trace was measured using a time domain reflectmetry (TDR) system (Agilent 86100A). The results of the Z_0 are shown in Fig. 3. The unit of the longitudinal axis is converted into impedance [Ω], after calibration by

50Ω at 0ns. Region before t=0.64ns is semi-rigid cable, and region after t=0.64ns is signal trace. The Z_0 are approximately 50Ω. The differences of the time of propagation result from the variation of effective dielectric constant.

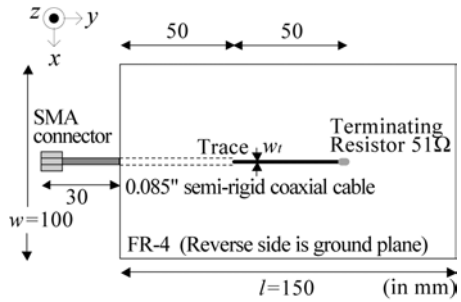

Fig. 1 Geometry of the PCB layout under test.

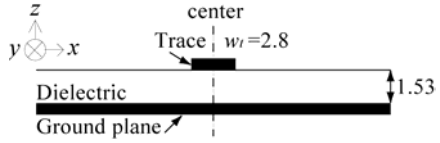

(a) Surface Micro-Strip Line structure (S-MSL)

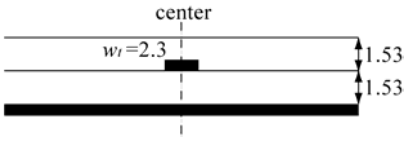

(b) Embedded Micro-Strip Line structure (E-MSL)

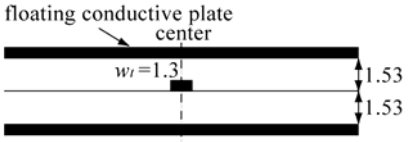

(c) Strip Line structure (SL)

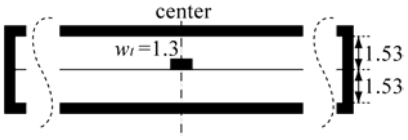

(d) Shield structure (Shield)

Fig. 2 Cross-sectional scheme of four kinds of structure (in mm).

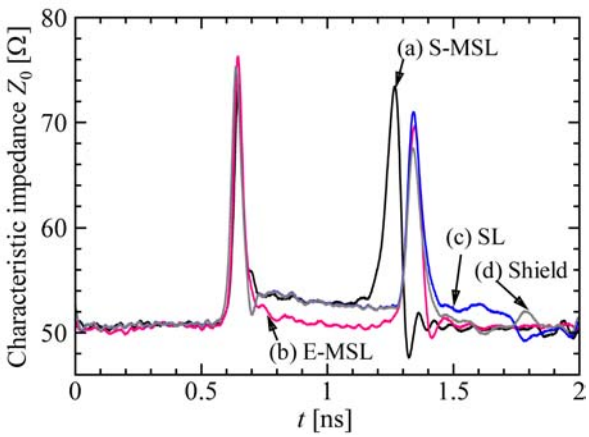

Fig, 3 Characteristic impedance Z_0 of the trace measured by TDR.

3. Experimental and Modeling Method for CM current

3.1 Experimental Method

The CM current on the outer shield of the signal feed cable was measured using a shielded-loop probe (SLP) [8], and a network analyzer (Agilent E8358A), as shown in Fig. 4. A 500x500mm^2 aluminum plate was used to isolate the PCB from the network analyzer. The $|S_{21}|$ at the location of Port 1 (the voltage source for the signal trace) and Port 2 (SLP on the semi-rigid cable) was measured in the frequency range from 100MHz to 3GHz. Port 1 was connected to the 0.085" coaxial cable to drive the signal line, and Port 2 was connected to the SLP. The 10dB attenuator was used to match the impedance of a SLP to a coaxial cable. The SLP signal is amplified by 40dB.

The calibration of the network analyzer and removal of the frequency response of the SLP were implemented [5]. The incident voltage at Port 2 is related to the CM current by $|V_2^-|=50|I_{CM}|$, where the source impedance of the network analyzer is 50Ω. The input voltage at Port 1 is $|V_1^+|=|V_S|/2$, where V_S is the source voltage of the network analyzer, since the source impedance is matched to the characteristic impedance of the cable. As $|S_{21}|$ is the ratio of the received voltage at Port 2 to the input voltage at Port 1, the relationship between the $|S_{21}|$ and CM current is given by

$$|S_{21}| = \frac{100|I_{CM}|}{|V_S|}. \qquad (1)$$

This is used to compare experimental and numerical results.

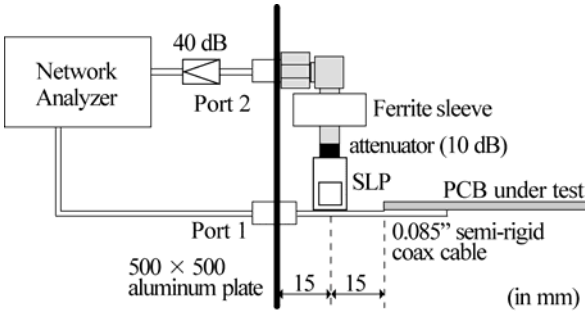

Fig. 4 Experimental setup for common-mode current measurement.

3.2 Method of FDTD Modeling

The FDTD method [9] is used for modeling CM current on a feed cable attached to the PCB. The FDTD modeling details were determined by varying the number of cells for trace width, substrate thickness, and the space between PCB and absorbing boundary condition (ABC) [4]. Perfectly matched layers (PMLs) [10], eight cells deep, were used as the ABC. The measured and simulated results were in good agreement when the meshing of the trace and the substrate was greater than two cells, and the

space between the PCB and PMLs was wider than λ/120, where λ was the wavelength of the lowest frequency interested. Therefore, calculation conditions were set up as shown in Table I. Figure 5 shows the computational domain for the FDTD simulation in the case of "S-MSL". The trace, ground plane and aluminum plate were modeled as perfect electric conductor. The aluminum plate used in the experiments was included as an infinite ground plane in the model. An SMT resistor was modeled as one cell lumped element in the PCB substrate. The PCB substrate was modeled as a dielectric with relative permittivity ε_r=4.5. A sinusoidally modulated Gaussian pulse was used as the source with source resistance 50Ω. The CM current was calculated from average magnetic field strength H_x in the SLP, where the SLP area was 9.2x9.2mm^2.

To shorten the calculation time, the vector and parallel computation method for a super computer (NEC SX-7) was used in FORTRAN 90, where IF-THEN operations in a vector loop were eliminated.

Table I Calculation conditions in FDTD modeling.

	Δx [mm]	NXxNYxNz
(a) S-MSL	0.467	311x114x220
(b) E-MSL	0.575	271x114x220
(c) SL	0.65	251x114x220
(d) Shield		

(Δy=2.5 and Δz =0.765mm, Δt=1.3ps, NXxNYxNZ is total computational domain)

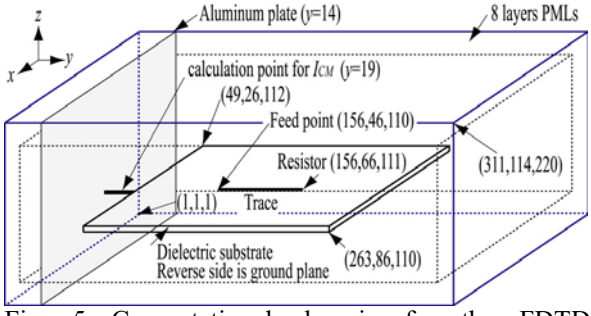

Fig. 5 Computational domain for the FDTD simulation. (ex. S-MSL)

4. Results and Discussions

4.1 Effect of PCB Structure on CM Current

The $|S_{21}|$ related to CM current is shown in Fig. 6. Solid lines and broken lines are measured and calculated results, respectively. The calculated and measured results are in good agreement. In all cases, first resonance frequency is 273MHz. In the case of "S-MSL" and "E-MSL", second resonance frequency is 860MHz. And the $|S_{21}|$ in the "E-MSL" case is almost the same as the "S-MSL" case. The resonance frequencies expect first resonance in the "SL" and "Shield" are lower than the resonance frequencies in the "S-MSL". This shift is due to conductive plate which exists near the signal trace. The resonance frequencies in the "SL" are 273, 482, 960, 1420MHz and so on. These frequencies except first resonance correspond to resonance frequencies depend on a power-ground layer resonator as the following Eq.(2)

$$f = \frac{150}{\sqrt{\varepsilon_r}} \sqrt{\left(\frac{m}{W}\right)^2 + \left(\frac{n}{l}\right)^2} \quad \text{[MHz]}, \qquad (2)$$

$$m = 0.1,2... \quad n = 0,1,2...$$

where m and n represent the mth and nth mode associated with x and y-dimensions, respectively. The calculated results with Eq. (2) are shown in Table II. The resonance frequencies correspond to resonance frequencies when (m,n)=(1,0), (2,0), (3,0) and so on. The difference between the case of "S-MSL" and "SL" at lower frequencies is approximately 6dB.

The shielded structure is more effective than other structures in suppressing the CM current. The difference between "S-MSL" and "Shield" case at the first resonance frequency is approximately 6dB. This is consistent with an EMI coupling path dominated by the magnetic field [2]. However, because conductive plate exists near the signal trace, $|S_{21}|$ in the "SL" and "Shield" cases yield resonances with high level peak. If the magnetic flux which encloses a ground plane decreases, the CM current decreases. In short, PCB structure which holds magnetic field into the dielectric and without conductive plate exists near the signal trace is required.

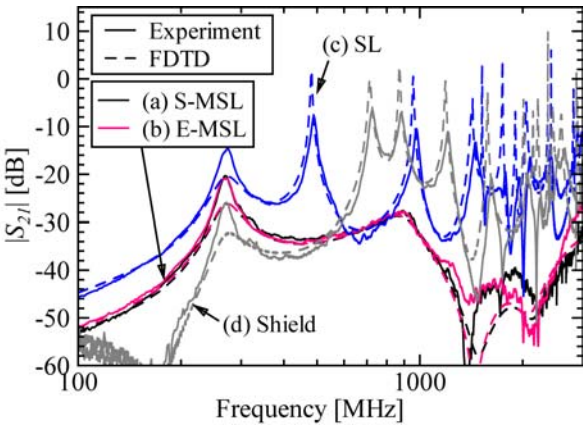

Fig. 6 Effect of PCB structure on CM current.

Table II Resonance frequencies [MHz] calculated by Eq. (2).

		m			
		0	1	2	3
n	0		707	1414	2121
	1	471	849	1490	2173
	2	942	1179	1700	2321
	3	1414	1581	2000	2549

4.2 Effect of PCB Structure on Reflection Coefficient

The reflection coefficient $|S_{11}|$ at a SMA connector was measured using a network analyzer (Agilent E8358A). The experimental results of $|S_{11}|$ are shown in Fig. 7. The resonance and antiresonance frequencies higher order than the first resonance equal to that of $|S_{21}|$ which related to CM current.

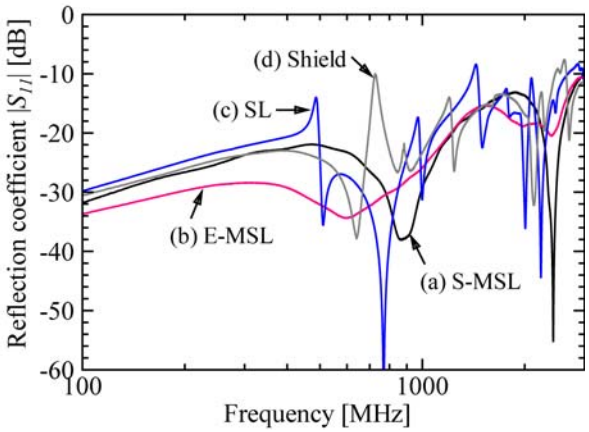

Fig. 7 Effect of PCB structure on the reflection coefficient $|S_{11}|$.

5. Conclusion

The effect of PCB cross sectional structure on CM current on feed cable is investigated with experiment and FDTD modeling. Four kinds of PCB structures, which are expected as typical structures, are used to compare. Results show that "Shield" is effective in suppressing the CM current at lower frequencies. However, because conductive plate exists near the signal trace, $|S_{21}|$ in the "SL" and "Shield" cases yield resonances with high level peak. A key feature of this study is as follows. Although the "SL" structure suppresses the direct radiation from the trace, "SL" may increase CM current. This study can be a basic consideration to realize a technique which is effective on the suppression of the CM current on the PCB with a connected feed cable.

In order to support these results, distinguishing between direct radiation from the trace and radiation as a result of the CM current in far-field should be the further studies.

Acknowledgments

The authors express their thanks to Prof. James L. Drewniak, University of Missouri-Rolla, USA, for his helpful discussions on this research, and the Information Synergy Center, Tohoku University, Sendai, Japan, for their support with computer resources. This research was partly supported by Collaboration of Regional Entities for the Advancement of Technological Excellence in Akita Prefecture.

References

[1] e.g., C.R. Paul, *Introduction to Electromagnetic Compatibility*, New York: John Wiley & Sons, 1991.

[2] D.M. Hockanson, J.L. Drewniak, T.H. Hubing, T.P. VanDoren, F. Sha and M.J. Wilhelm, "Investigation of Fundamental EMI Source Mechanisms Driving Common Mode Radiation from Printed Circuit Boards with Attached Cables", *IEEE Trans. Electromagn. Compat.*, vol.38, no.4, pp.557-576, Nov. 1996.

[3] M. Leone, "Design Expressions for the Trace-to Edge Common-Mode Inductance of a Printed Circuit Board", *IEEE Trans. Electromagn. Compat.*, vol.43, no.4, pp.667-671, Nov. 2001.

[4] Y. Kayano, M. Tanaka and H. Inoue, "A Simulation of Common-Mode Current on a Semi-rigid Cable Attached to a PCB (in Japanese)", IEICE Technical Report, EMD2001-1, Apr. 2001.

[5] Y. Kayano, M. Tanaka, J.L. Drewniak and H. Inoue, "A Study on Influence of Guard-Band on Common-Mode Current related to a Microstrip Line", IEEE Int. Symp. Electromagn. Compat. (Istanbul, Turkey), TH-A-I3.5, May 2003.

[6] D.M. Pozer, *Microwave Engineering 2nd Ed.*, John Wiley & Sons, 1998.

[7] K. Otsuka, C. Ueda, Y. Odate, T. Usami and T. Suga, "Study of beyond GHz Signal Integrity under TEM Wave Mode Analysis in Multi-channel Transmission Lines", Proc. 2002 *Int. Conf. Electronics Packaging* (Tokyo, Japan), pp.295-300, Apr. 2002.

[8] M. Yamaguchi, S. Yabukami and K.I. Arai, "A New Permeance Meter Based on Both Lumped Elements/Transmission Line Theories", *IEEE Trans. Magn.*, vol.32, no.5, pp.4941-4943, Sep. 1996.

[9] A. Taflove, *Computational Electrodynamics; The Finite-Difference Time-Domain Method*, Norwood, MA: Artech House, 1995.

[10] J.P. Berenger, "Three-Dimensional Perfectly Matched Layer for the Absorption of Electromagnetic Waves"', *J. Computational Physics*, vol.127, pp.363-379, 1996.